

Linear bases for representation of natural and artificial illuminants

Javier Romero, Antonio García-Beltrán, and Javier Hernández-Andrés

Department of Optics, Faculty of Sciences, University of Granada, 18071 Granada, Spain

Received December 8, 1995; accepted October 17, 1996; revised manuscript received November 14, 1996

By the principal-value decomposition process, we have obtained two linear bases for representing the spectral power distributions of illuminants, applicable for algorithms of color synthesis and analysis in artificial vision: one from experimental measurements of daylight and another combining both natural and artificial illuminants. The first basis adequately represents daylight with dimension 3, in accordance with the previous results of Judd *et al.* [J. Opt. Soc. Am. **54**, 1031 (1964)]; however, it does not adequately represent artificial illuminants, even with a higher dimension. In the case of the second basis, many good results are obtained in the reconstruction of the spectral power distribution both of daylight and of artificial illuminants, including some fluorescent lights, with dimension 7 or even less. In consequence, we show the possibility of obtaining linear bases of a low dimension, even when the set of illuminants that we try to represent presents a certain variability in shape. © 1997 Optical Society of America [S0740-3232(97)00905-8]

1. INTRODUCTION

Research on methods of color analysis and synthesis has often dealt with linear models for representing illuminants, which, together with those of reflectance representation, permit the design of algorithms applicable in artificial vision (see, e.g., Maloney and Wandell¹ and Wandell²). These models are intended to establish a basis for representing the spectral power distribution of the illuminants in reduced dimensions. The basis is formed by a group of characteristic vectors obtained after carrying out a principal-value decomposition process on experimental measurements of spectral power distributions.

In this field the references center on the works of Judd *et al.*³ and Dixon.⁴ These authors studied the spectral energy distribution of daylight in the visible spectrum and concluded in a general way that three characteristic vectors are sufficient to produce a basis for the appropriate representation of this type of radiation. Other authors investigating this field have drawn similar conclusions.^{5,6}

Nevertheless, we believe that adopting a representational basis obtained for daylight when working in artificial vision is not useful at all. Often, we find ourselves under artificial lighting conditions and have no assurance that the illuminants used can be adequately represented over a basis that was established for natural light. We might ask whether the bases deduced for the daylight would serve under lighting conditions normally used in artificial vision.

Thus the objectives of the present work are as follows: first, to study the applicability of a daylight basis to represent artificial illuminants; second, to obtain a representational basis that includes both natural illuminants and artificial ones; and, finally, to study the appropriate dimension of this basis and its possibilities for representing a variety of illuminants, among these being those proposed by the CIE. For this purpose we carried out our own principal-value decomposition process; first on mea-

surements appropriate to daylight and then over a wide group of spectral power distributions that included both daylight and artificial illuminants.

2. METHOD

The analytic methods used here are described in Parkkinen *et al.*⁷ The data were analyzed by using the Karhunen-Loève transformation.

If we have a group of spectral power distributions $E_e(\lambda)$ and we wish to obtain the set of eigenvectors associated with the group, first we must obtain the correlation matrix $R_{\mathcal{T}}(E)$ to diagonalize it later. In our analysis, to obtain this matrix, we first had to normalize each spectral power distribution by the Euclidean rule,

$$E(\lambda_i) = \frac{E_e(\lambda_i)}{\left\{ \sum_j [E_e(\lambda_j)]^2 \right\}^{1/2}}, \quad (1)$$

so that our study was not influenced by the possible variability in the absolute values of the spectral power distributions selected.

From each curve measured, we obtained the symmetric matrix R_{ij} through the inner product:

$$R_{ij} = E(\lambda_i)E(\lambda_j), \quad \lambda_i = 395 + i5 \text{ nm}, \\ \lambda_j = 395 + j5 \text{ nm}, \quad (2)$$

where $1 \leq i, j \leq 61$; then we took spectral power distribution values from 400 to 700 nm at 5-nm intervals.

Adding together all the symmetric matrices, each one calculated for a spectral power distribution, we obtained the correlation matrix $R_{\mathcal{T}}(E)$.

Afterward, we submitted $R_{\mathcal{T}}(E)$ to a principal-value decomposition process and obtained its eigenvalues and eigenvectors. We normalized all the eigenvectors and sorted them according to decreasing eigenvalues; this al-

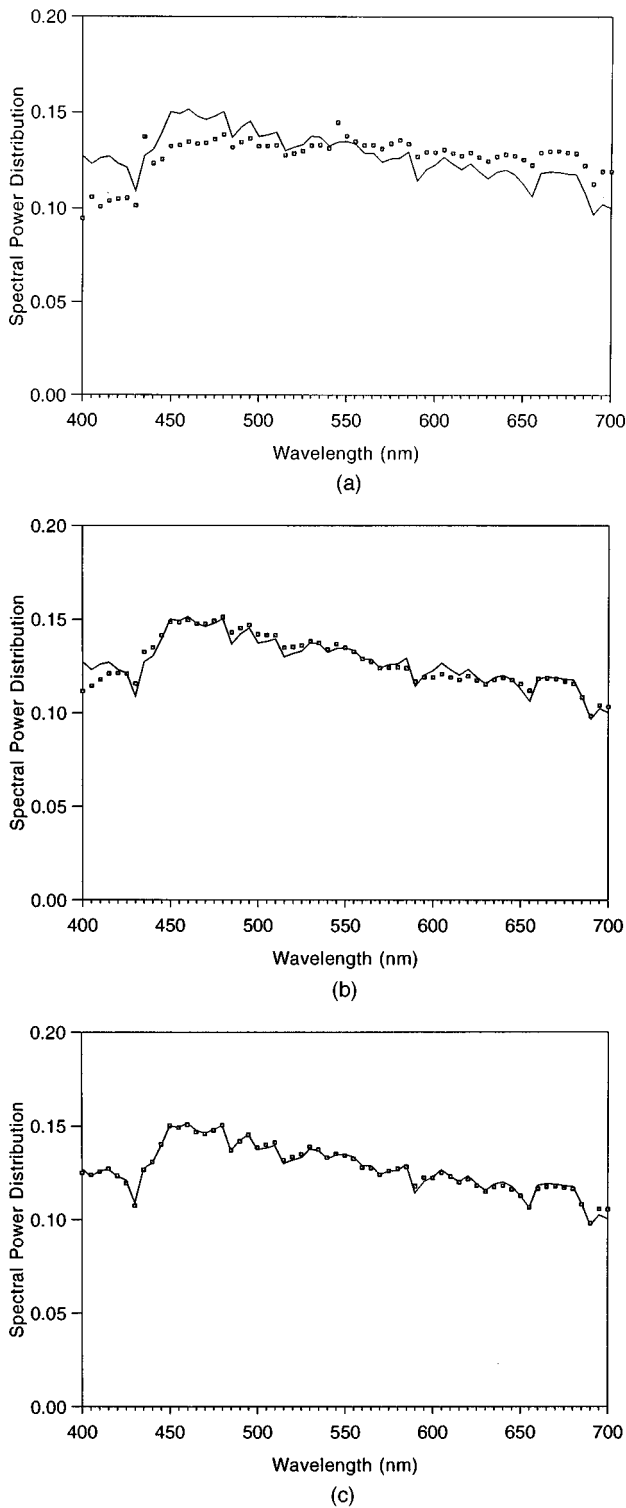


Fig. 1. Example of reconstruction with (a) a GFC of 0.995688, (b) a GFC of 0.999566, (c) a GFC of 0.999939. Solid curve: original curve; points: reconstruction.

lowed us to determine which eigenvector contributed the most strength to the basis generation.

For the mathematical reconstruction of a spectral power distribution $E(\lambda)$, we used the formula

$$E_a(\lambda) = \sum_{n=1}^p \langle E(\lambda)|V_n(\lambda)\rangle V_n(\lambda), \quad (3)$$

where $E_a(\lambda)$ is the reconstructed spectral power distribution, $\langle E(\lambda)|V_n(\lambda)\rangle$ is the usual inner product (scalar product) between the spectral power distribution and the n -basis eigenvector $V_n(\lambda)$, and p is the number of eigenvectors with which we wish to recover the spectral distribution.

To evaluate the goodness of the mathematical reconstruction, we used a goodness-fitting coefficient (GFC), based on the inequality of Schwartz:

$$\text{GFC} = \frac{\left| \sum_{j=1}^{61} E(\lambda_j)E_a(\lambda_j) \right|}{\left[\sum_{j=1}^{61} [E(\lambda_j)]^2 \right]^{1/2} \left[\sum_{j=1}^{61} [E_a(\lambda_j)]^2 \right]^{1/2}},$$

$$\lambda_j = 395 + j5 \text{ nm}, \quad (4)$$

where $1 \leq j \leq 61$. This GFC is just the multiple correlation coefficient R and the square root of the variance-accounted-for coefficient (VAF). The values of the GFC range from 0 to 1, where 1 indicates a perfect reconstruction. If the reconstructed spectral power distribution $E_a(\lambda)$ were normalized to unit length, the GFC would be the cosine of the angle between E and E_a , both considered as vectors in a space of dimension 61.

Figure 1 provides examples of values that took this coefficient when we reconstructed the spectral power distribution of a source with different numbers of vectors from the basis. When the reconstruction presented a $\text{GFC} \geq 0.99$, we judged the quality to be acceptable, especially from the standpoint of colorimetry. If the GFC obtained was ≥ 0.999 , the reconstruction was considered very good; and if it was ≥ 0.9999 , it was mathematically almost exact.

We have been interested in studying the goodness of the reconstruction from a functional viewpoint instead of a colorimetric point of view. Table 1 shows the chromaticity coordinates of the three examples of reconstruction in Fig. 1, which give an idea of the color differences found in the reconstructions.

A GFC of 0.90 (VAF of 0.81) can be considered as the 19% of the energy that is missed in the reconstruction. With this interpretation a GFC of 0.99 means that 2% is missed, a GFC of 0.999 corresponds to 0.2% missed, and a GFC of 0.9999 corresponds to 0.02% missed. As we can observe, at a level of 0.02% of energy missed, it may seem that we are worried about negligibly small errors. However, we wanted to be very strict in the reconstruction,

Table 1. Chromaticity Coordinates of the Three Examples of Reconstructions Shown in Fig. 1

GFC	Original	Reconstructed
0.995688	$x = 0.3197$ $y = 0.3295$	$x = 0.3332$ $y = 0.3405$
0.999566	$x = 0.3197$ $y = 0.3295$	$x = 0.3169$ $y = 0.3293$
0.999939	$x = 0.3197$ $y = 0.3295$	$x = 0.3194$ $y = 0.3302$

Table 2. Atmospheric Conditions of the Days on Which the Experimental Measurements Were Taken

Day	Atmospheric Conditions		Number of Measurements
Day 1, 4/8/95	Morning	Clear	25
	Evening	Clear	
Day 2, 4/11/95	Morning	Cloudy, rain	25
	Evening	Cloudy, rain	
Day 3, 4/13/95	Morning	Clear	24
	Evening	Cloudy	
Day 4, 4/15/95	Morning	Clear, misty	25
	Evening	Cloudy, misty	

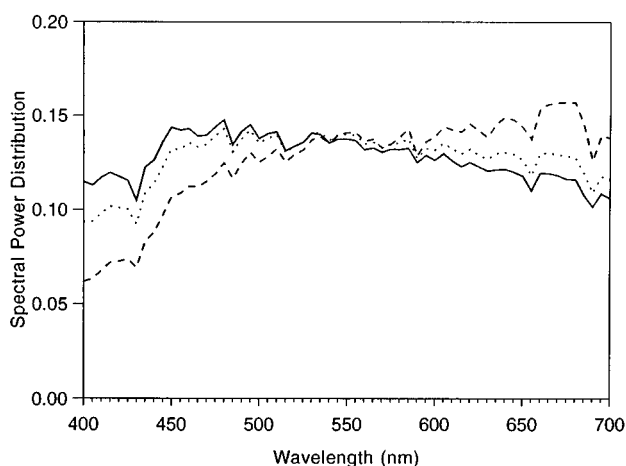


Fig. 2. Spectral power distribution of some experimental daylight measurements.

and for that reason we adopted the three categories described above. In this way we fixed the dimension of the basis that allowed the representation of a group of illuminants.

3. EXPERIMENTAL MEASUREMENTS AND DAYLIGHT BASIS

First, we tried our method on daylight measurements and compared our results with those of other authors.³⁻⁶ We have to point out that we have not had the objective to cast doubt on the results of Judd *et al.*³ for a daylight representation, results that are well established and have been widely adopted by the scientific community. We wanted to obtain our own set of daylight experimental measurements and its linear basis representation so as to supplement it later with the artificial illuminants spectral power distributions and, in this way, to construct a common basis for both sets of data.

For this purpose we made a series of experimental measurements of daylight in Granada, Spain (latitude 37°11' N, longitude 3°35' W, altitude 680 m) for four days during the month of April 1995. Table 2 shows the atmospheric conditions each day and the number of mea-

surements carried out inclusively from sunrise to sunset at periodic intervals of 30 min.

The experimental measurements were made by using a white Lambertian receptor with a flat spectral reflectance of between 400 and 700 nm, which we situated facing the Sun, and an SR-1 Topcon spectroradiometer (Topcon Europe B.V., Rotterdam), with which we measured the light reflected by the white receptor at 45° to its perpendicular. Therefore the geometry of the measurements was 0/45°. In this way we made indirect measurements of daylight (direct plus the light from the sky), since the spectral irradiance was proportional to the spectral radiance measured on the receptor, thus accomplishing the objectives of the present work. With this geometry we measured sunlight plus skylight, eliminating the specular component of sunlight. When the sky was covered with clouds, we obviously measured only the radiation from the sky.

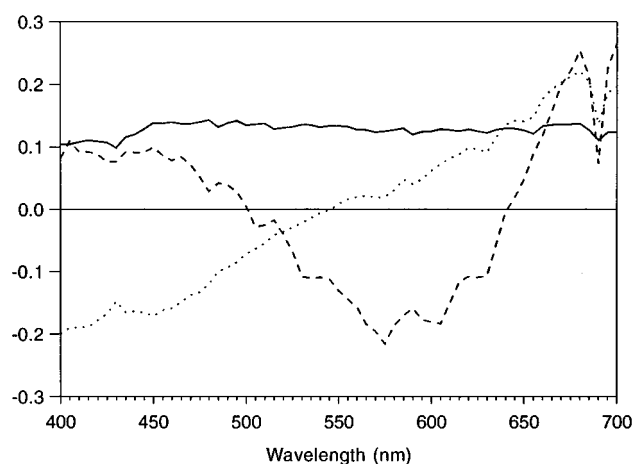


Fig. 3. Spectral profile of the first three eigenvectors of the basis of experimental measurements. Solid curve: eigenvector 1; dotted curve: eigenvector 2; dashed curve: eigenvector 3.

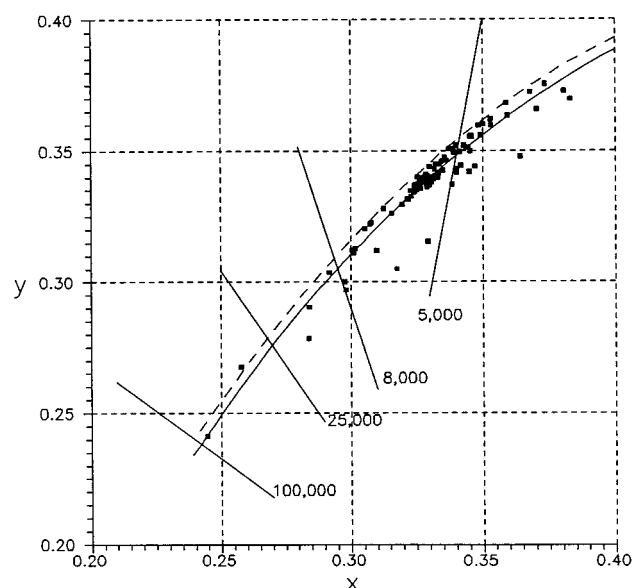


Fig. 4. Chromaticity coordinates of daylight measurements in Granada, and Planckian locus (solid curve) and CIE daylight locus (dashed curve).

Table 3. GFC Obtained in Each of the Standard CIE Illuminants with the Global Basis and the Basis of Experimental Measurements with Use of Different Numbers of Vectors

Standard CIE Illuminants	GFC			
	Global Basis	(No. of Vectors)	Basis of Experimental Measurements	(No. of Vectors)
A	0.990342	(3)	0.993925	(3)
	0.999425	(4)	0.996868	(4)
	0.999528	(7)	0.999195	(7)
	0.999965	(10)	0.999289	(10)
B	0.998202	(3)	0.998268	(3)
	0.998590	(4)	0.998389	(4)
	0.999927	(7)	0.998935	(7)
	0.999981	(10)	0.999059	(10)
C	0.996222	(3)	0.996258	(3)
	0.997254	(4)	0.996651	(4)
	0.999963	(7)	0.997512	(7)
	0.999994	(10)	0.997816	(10)
D ₅₅	0.998601	(3)	0.999333	(3)
	0.998661	(4)	0.999735	(4)
	0.999847	(7)	0.999754	(7)
	0.999993	(10)	0.999777	(10)
D ₆₅	0.998261	(3)	0.999540	(3)
	0.999657	(4)	0.999747	(4)
	0.999850	(7)	0.999756	(7)
	0.999991	(10)	0.999777	(10)
F ₂	0.943412	(3)	0.902988	(3)
	0.997532	(4)	0.906935	(4)
	0.999822	(7)	0.960598	(7)
	1.000000	(10)	0.962187	(10)
F ₇	0.977805	(3)	0.927684	(3)
	0.984056	(4)	0.927935	(4)
	0.999831	(7)	0.949162	(7)
	1.000000	(10)	0.954743	(10)
F ₁₁	0.977489	(3)	0.633774	(3)
	0.999904	(4)	0.635411	(4)
	1.000000	(7)	0.706311	(7)
	1.000000	(10)	0.724624	(10)

It should be mentioned that we did not attempt an exhaustive characterization of daylight or its absolute values in Granada; rather, we sought a variety of spectral distribution curves corresponding to different phases of daylight and varying meteorological conditions, which allowed us to obtain a highly representative basis to achieve our objective. Figure 2 presents some examples of the daylight spectral distributions obtained.

The first three eigenvectors obtained for the group of 99 spectral distributions, which we use to generate the first basis, called the basis of experimental measurements, are shown in Fig. 3. The first eigenvector corresponds to the mean of the spectral distributions contributing to the correlation matrix. This presents a roughly flat profile with lower values toward the ends of the spectrum, as found by other authors.³⁻⁶

The second and third vectors varied with the wavelength, proving sensitive to yellow-blue and pink-green

variations in daylight, in agreement with the results shown by Judd *et al.*³ and Sastri and Das.⁵

The chromaticity coordinates computed from our data are shown in Fig. 4. As we can observe, most of them are located near the Planckian locus, with correlated color temperatures between 4500 and 7000 K, in overall agreement with the results of other authors.³⁻⁶

In our case the first three eigenvectors of the basis of experimental measurements accounted for 99.97% of the variance. With the first three eigenvectors, 100% of the 99 curves obtain a GFC > 0.99, 97.98% obtain a GFC ≥ 0.999, and 62.63% obtain a GFC ≥ 0.9999. We obtain the worst representations for the sunrise and sunset measurements, with a minimum GFC of 0.9977. The reconstruction of our 99 experimental daylight measurements with the first three eigenvectors of the basis of experimental measurements provided an average GFC of 0.999825, which represents a very good fit. For this reason we con-

cluded, in agreement with Judd *et al.*,³ that 3 is an appropriate dimension for the basis obtained for representations of these types of measurement.

However, we might ask what occurs when we attempt to represent, with this basis, spectral power distributions different from those used in generating the correlation matrix. Let us examine the situation in which we try to reconstruct mathematically the D_{65} illuminant, artificial illuminants such as the A illuminant, or a fluorescent one such as F_2 .

In column 3 of Table 3, the GFC's obtained are shown for the three above illuminants with different numbers of vectors of the basis. As can be seen, good results are gained with three vectors for the D_{65} illuminant. Nevertheless, for other daylight-type illuminants, such as C, the results are not as good, even with seven eigenvectors.

For illuminant A seven vectors were necessary for a reconstruction comparable with that of the D_{65} , and, in the case of the fluorescent illuminants, no acceptable reconstruction was achieved, even with a greater number of vectors. This might be expected, given the peculiarities of the fluorescent illuminants, with emission peaks at some wavelengths corresponding to spectral lines of certain elements.

If we wish to establish, with few parameters, a basis that represents a greater quantity of illuminants, we must include in the correlation matrix either those that we seek to represent or spectral-emission characteristics similar to those that were included. Therefore, in the following section, we describe how we obtained a basis that served to represent a variety of illuminants, both natural and artificial, with a dimension as reduced as possible.

4. GLOBAL BASIS

To generate this basis, we created the correlation matrix from 48 daylight spectral distributions (chosen from among our measurements), seven spectral power distribution curves from the blackbody of temperatures (2000, 3000, 4000, 5000, 6000, 7000, and 8000 K), and seven distributions corresponding to standard illuminants of the CIE (B, C, D_{55} , D_{65} , F_2 , F_7 , and F_{11}). We used three of the standard CIE fluorescent illuminants that represent the general characteristics of fluorescent sources: standard (F_2), broadband (F_7), and three narrow-band (F_{11}), as recommended by the CIE⁸ from 380 to 780 nm at 5-nm intervals. The latter seven spectral distributions were introduced into the matrix three times (that is, with weight 3). In this way we sought a certain equilibrium between distributions of the daylight-type measurements and the rest of the illuminants used.

The graphical representation of the first ten eigenvectors is shown in Fig. 5. The inclusion of fluorescent illuminants caused the eigenvectors to lose smoothness.

In Table 3 we have added the GFC obtained on testing the global basis with the use of different standard illuminants. As can be seen, the global basis adequately represented all the illuminants tested, both daylight and artificial, with dimension 7, even improving the one obtained by the basis of experimental measurements for daylight-type illuminants.

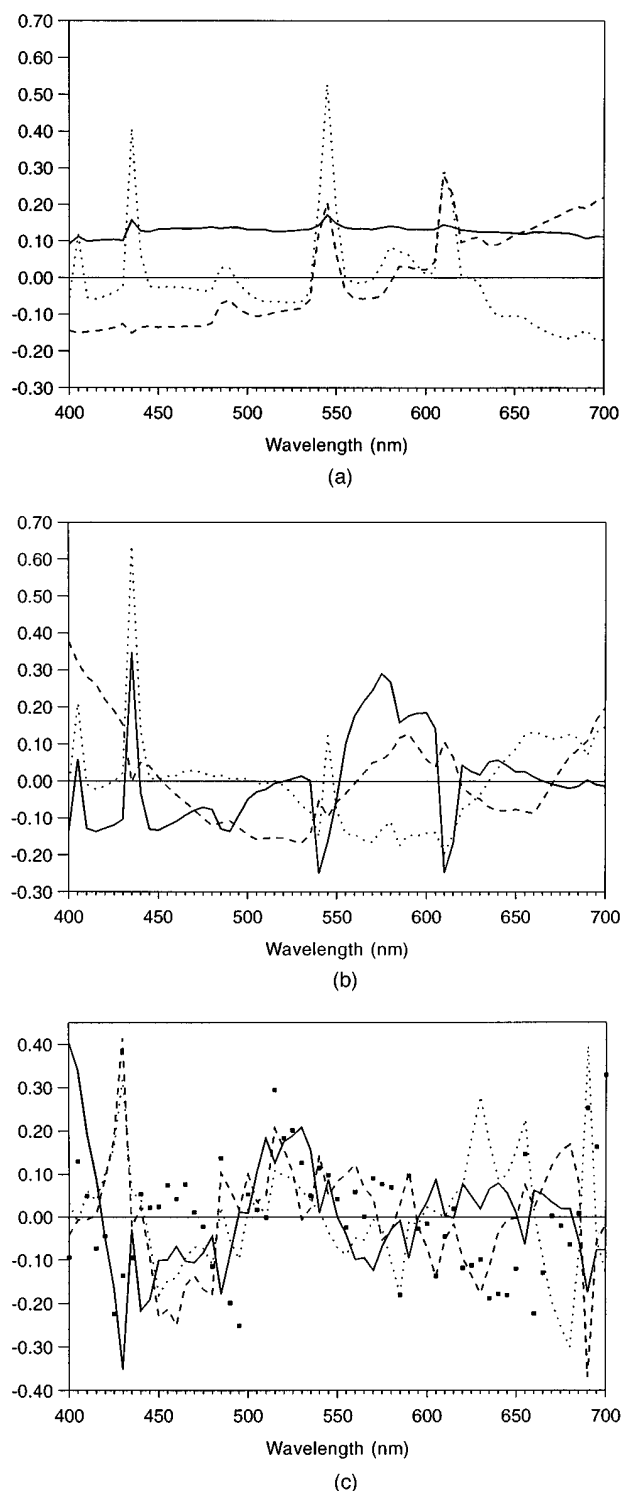


Fig. 5. Spectral profile of the first six eigenvectors of the global basis. (a) Eigenvectors 1 to 3. Solid curve: eigenvector 1; dotted curve: eigenvector 2; dashed curve: eigenvector 3. (b) Eigenvectors 4 to 6. Solid curve: eigenvector 4; dotted curve: eigenvector 5; dashed curve: eigenvector 6. (c) Eigenvectors 7 to 10. Solid curve: eigenvector 7; dotted curve: eigenvector 8; dashed curve: eigenvector 9; points: eigenvector 10.

Thus we can state that four eigenvectors make it possible with the global basis to reconstruct quite satisfactorily the illuminants A, D_{65} , F_2 , and F_{11} , which is graphi-

cally illustrated in Figs. 6(a), 6(b), 6(c), and 6(d), respectively.

Our aim was to test the basis obtained with illuminants whose spectral-emission curves were not used in the generation of the basis. The results for illuminant A, as shown above, can be considered highly satisfactory, as might be expected, since this illuminant corresponds to the blackbody of temperature 2856 K and therefore with a spectral power distribution very similar to the blackbody of 3000 K introduced into the correlation matrix.

In addition, good results are achieved for this illuminant when it is reconstructed with the daylight basis. The explanation is that our experimental daylight measurements presented color temperatures of between 2000 and 8000 K as well as chromaticity coordinates very near or over the blackbody locus in the CIE 1931 chromatic diagram, as in the results of other authors.³⁻⁶

When we tried the global basis with daylight spectral distributions measured by us (but not included in the correlation matrix) with three eigenvectors, we attained a reconstruction whose GFC was consistently greater than 0.9990. Nevertheless, with the use of other illuminants, such as the blackbody for temperatures above and below

those used in the generation of the basis, the results were not as good. Thus, whereas for a temperature of 10,000 K a GFC of 0.998933 was obtained by reconstructing with seven eigenvectors with equal dimension, the GFC obtained for 1000 K was 0.973258.

For the tests of the fluorescent illuminants, the results again were diverse. Whereas for the standard F₃ illuminant, we obtained a GFC of 0.999304 in a reconstruction with seven eigenvectors [Fig. 7(a)], for the other standard fluorescent illuminants with this dimension, the GFC values, although in an acceptable reconstruction category, do not reach 0.999. However, in Fig. 7(b) and 7(c), we show representative examples in which we can consider the reconstructions to be quite adequate, especially for colorimetric purposes.

Last, for the reconstruction of the spectral power distribution of one commercial fluorescent tube [Fig. 7(d)], the results again, though acceptable, cannot be considered completely satisfactory. We should mention that although, to generate the correlation matrix, we used three standard CIE fluorescent illuminants⁸ that represent the general characteristics of fluorescent sources, it is difficult with our analysis to accommodate the complete commer-

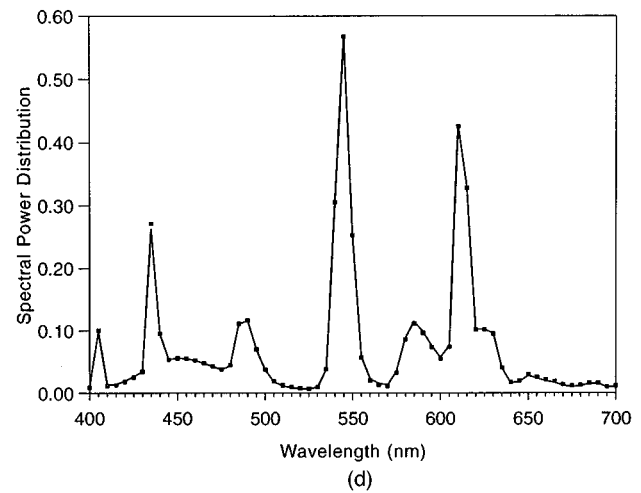
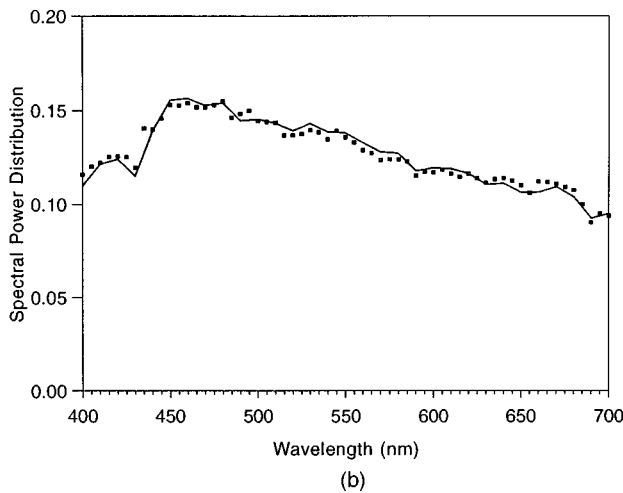
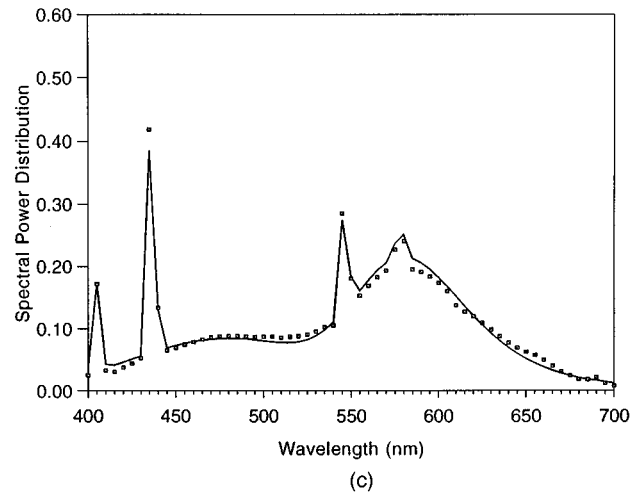
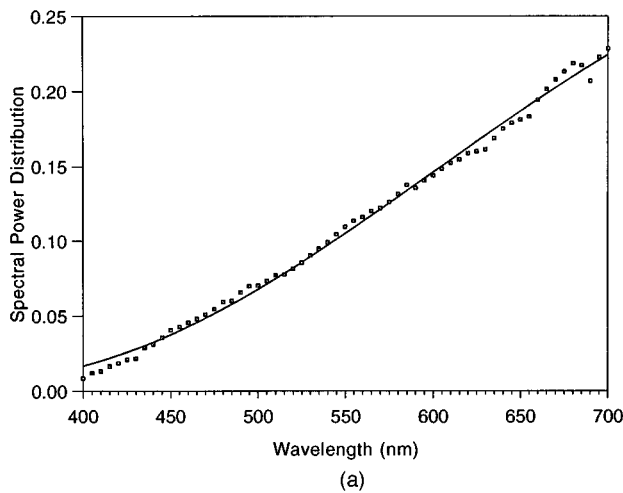


Fig. 6. Examples of reconstructions of some standard CIE illuminants using four vectors of the global basis. (a) Illuminant A. GFC = 0.999425. Solid curve: illuminant A; points: reconstruction. (b) Illuminant D₆₅. GFC = 0.999657. Solid curve: illuminant D₆₅; points: reconstruction. (c) Illuminant F₂. GFC = 0.997532. Solid curve: illuminant F₂; points: reconstruction. (d) Illuminant F₁₁. GFC = 0.999904. Solid curve: illuminant F₁₁; points: reconstruction.

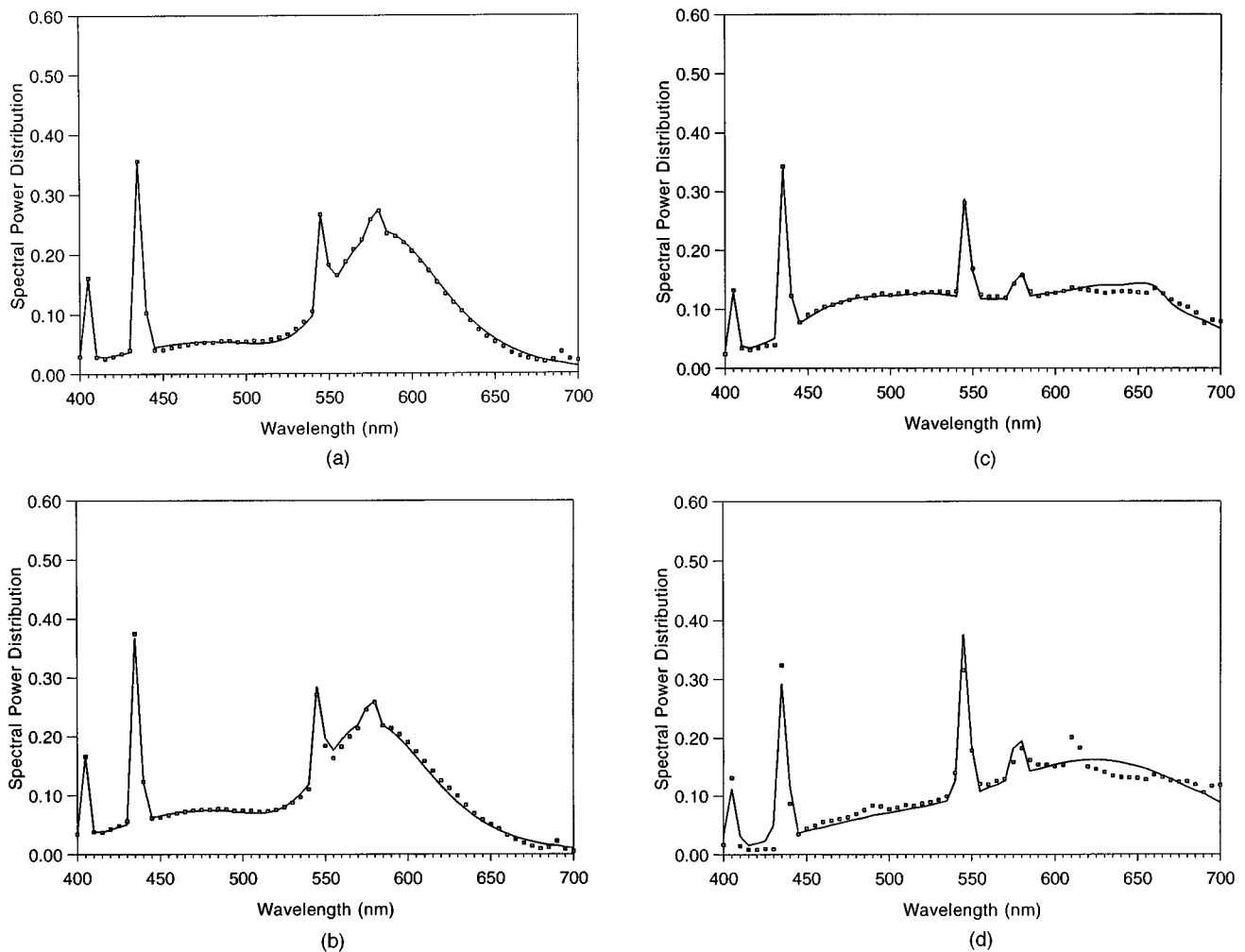


Fig. 7. Examples of reconstructions of some fluorescent illuminants using the global basis. (a) Illuminant F_3 with seven eigenvectors. GFC = 0.999304. Solid curve: illuminant F_3 ; points: reconstruction. (b) Illuminant F_6 with seven eigenvectors. GFC = 0.998886. Solid curve: illuminant F_6 ; points: reconstruction. (c) Illuminant F_8 with seven eigenvectors. GFC = 0.998660. Solid curve: illuminant F_8 ; points: reconstruction. (d) Commercial fluorescent tube with seven eigenvectors. GFC = 0.991128. Solid curve: commercial fluorescent tube; points: reconstruction.

cial diversity of this type of light source, particularly if the goal is a basis with reduced dimension. We would like to make it clear that our purpose was not to generate a basis that could represent every kind of illuminant but to try to lay the foundations of the method to follow when we need a basis for adequately representing a certain set of illuminants.

5. CONCLUSIONS

We have shown how a representational basis, obtained with daylight spectral power distributions, presents difficulties for the representation of artificial illuminants. This occurs both with dimension 3 and higher ones, although exceptions can be found (illuminant A).

In general, with the basis obtained on including in the correlation matrix both natural and artificial illuminants, dimension 4 provides a good reconstruction of the illuminants used. Nevertheless, if our basis is to represent other illuminants, we must increase to dimension 7 in order to obtain what we have considered to be good reconstructions.

As a general conclusion, it can be said that if we wish to obtain a low-dimension basis, but one that represents a wide variety of illuminants, both natural and artificial, these should be included, as far as possible, in the correlation matrix of the one that generates the basis. In any case the dimension necessary will be greater than 3.

ACKNOWLEDGMENTS

This research was supported by the Dirección General de Investigación Científica y Técnica, Ministerio de Educación y Ciencia, Spain, under grant PB91-0717. Also, we thank Laurence T. Maloney, whose comments greatly helped to improve this paper.

REFERENCES

1. L. T. Maloney and B. A. Wandell, "Color constancy: a method for recovering surface spectral reflectance," *J. Opt. Soc. Am. A* **3**, 29–33 (1986).
2. B. A. Wandell, "The synthesis and analysis of color images," *IEEE Trans. Patt. Anal. Machine Intell.* **PAMI-9**, 2–13 (1987).

3. D. B. Judd, D. L. MacAdam, and G. Wyszecki, "Spectral distribution of typical daylight as a function of correlated color temperature," *J. Opt. Soc. Am.* **54**, 1031–1040 (1964).
4. E. R. Dixon, "Spectral distribution of Australian daylight," *J. Opt. Soc. Am.* **68**, 437–450 (1978).
5. V. D. P. Sastri and S. R. Das, "Typical spectral distributions and color for tropical daylight," *J. Opt. Soc. Am.* **58**, 391–398 (1968).
6. V. D. P. Sastri and S. B. Manamohan, "Spectral distribution and colour of north sky at Bombay," *J. Phys. D* **4**, 381–386 (1971).
7. J. P. S. Parkkinen, J. Hallikainen, and T. Jaaskelainen, "Characteristic spectra of Munsell colors," *J. Opt. Soc. Am. A* **6**, 318–322 (1989).
8. *Colorimetry*, 2nd ed., CIE Publ. 15.2 (Central Bureau of the CIE, Vienna, 1986), pp. 70–72.